ACS APPLIED MATERIALS & INTERFACES

Research Article

Cite This: ACS Appl. Mater. Interfaces 2018, 10, 1728−1733

www.acsami.org

# Amine-Modulated/Engineered Interfaces of NiMo Electrocatalysts for Improved Hydrogen Evolution Reaction in Alkaline Solutions

Wei Gao,[†,‡,§] Wangyan Gou,[†] Xuemei Zhou,[†] Johnny C. Ho,[*,‡,§,∥] Yuanyuan Ma,[*,†] and Yongquan Qu[*,†]

[†]Center for Applied Chemical Research, Frontier Institute of Science and Technology, and Shaanxi Key Laboratory of Energy Chemical Process Intensification, School of Chemical Engineering and Technology, Xi'an Jiaotong University, Xi'an 710049, P. R. China

[‡]Department of Materials Science and Engineering and [∥]State Key Laboratory of Millimeter Waves, City University of Hong Kong, 83 Tat Chee Avenue, Kowloon 999077, Hong Kong

[§]Shenzhen Research Institute, City University of Hong Kong, Shenzhen 518057, P. R. China

Supporting Information

**ABSTRACT:** The interface between electrolytes and electrocatalysts would largely determine their corresponding activity and stability. Herein, modulating the surface characteristics of NiMo nanoparticles by various adsorbed amines gives the tunability on their interfacial properties and subsequently improves their catalytic performance for hydrogen evolution reaction (HER) in alkaline solutions. Diamines can significantly improve their HER activity by decreasing the charge-transfer resistance and modulating the electronic structures of interfacial active sites. Importantly, among various amines, ethylenediamine facilitates the HER activity of NiMo with a remarkable decrease of 268 mV in the overpotential to reach 10 mA $cm^{-2}$ as compared with that of the unmodified NiMo in 1.0 M KOH. This method provides a novel strategy of regulating the interfacial properties to strengthen the catalytic performance of electrocatalysts.

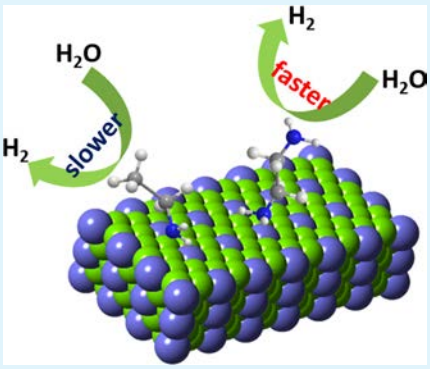


**KEYWORDS:** *hydrogen evolution, surface modulation, interface engineering, NiMo, electrocatalysis*

## 1. INTRODUCTION

Hydrogen production through electrochemical water splitting represents an efficient and crucial pathway for sustainable energy storage, which can not only benefit the distribution efficiency of the power grid but also at the same time provide useful chemicals and green fuels.[1,2] In this regard, in the past decade, heterogeneous catalysts based on earth-abundant elements have been widely explored and developed for both hydrogen evolution reaction (HER) and oxygen evolution reaction.[3−8] To further improve their catalytic HER performance, great efforts have been invested in controlling the electronic structures of the surface active sites through the modulations of morphology, constituent compositions, and/or dopants.[9−15] Also, regulating the surface-adsorbed species may provide an alternative approach to fine-tune the interfacial properties and the electronic structures of active materials.[16−19]

In general, electrocatalysts covered with adsorbed species would get their catalytic activity degraded because of the blockage of active surface sites.[17,18] For example, removal of the adsorbed oleylamine ligands on the Pt surface has been revealed to significantly improve its oxygen reduction activity.[17] However, the adsorbed species are also demonstrated with the potential to modify the electronic structures and then to promote the electrocatalytic activity of the active surface centers. In particular, the enhanced performance of the electrocatalysts modified by amines for formic acid oxidation and electrooxidation of nitric oxide and supercapacitor has been reported.[20−22] The surface engineering is well-illustrated to alter the surface wettability, to improve the accessibility of the reactants, and to enhance the electrochemical activity of the catalysts.[23−28] In any case, as compared with the exploration for other catalytic reactions, there is a very limited understanding on the surface modification of solid catalysts by the adsorbed species for HER.

Among many catalyst choices, nickel−molybdenum (NiMo) alloys have been extensively investigated as low-cost substitutions of high-performance noble-metal-based electrocatalysts for HER in alkaline media.[29−31] However, their corresponding catalytic activity is still unsatisfied until now. Herein, we report to utilize amine-modulated/engineered interfaces of NiMo electrocatalysts for improved HER in alkaline solutions. It is found that primary amines hinder the HER activity, whereas diamines promote the activity significantly. The diamine modification can engineer the interfacial properties of NiMo by decreasing the charge-transfer resistance and modulating the electronic structures of the

Received: October 24, 2017
Accepted: December 28, 2017
Published: December 28, 2017




DOI: 10.1021/acsami.7b16125
ACS Appl. Mater. Interfaces 2018, 10, 1728−1733

interfacial active sites. Explicitly, ethylenediamine (EDA) decoration can yield the best HER activity of NiMo with the lowest overpotential (72 mV) to drive the current density of 10 mA $cm^{-2}$, which is 268 mV lower than that of the unmodified NiMo. Therefore, surface engineering by decorating small molecules of amines on NiMo can regulate their interfacial properties with electrolytes and enhance their activity, deepening further insights into the relationship between small molecules and surface properties on the HER activity.

## 2. EXPERIMENTAL SECTION

**2.1. Synthesis of NiMo Electrocatalysts.** NiMo nanoparticles were synthesized using a modified precipitation method.[29] Briefly, to prepare NiMo precursors, 1 mmol $Ni(NO_3)_2{\cdot}6H_2O$ and 0.143 mmol $(NH_4)_6Mo_7O_{24}{\cdot}4H_2O$ were dissolved in 1 mL of deionized water with stirring in a 20 mL vial. Then, 0.4 mL of ammonia solution (25−28%) and 9 mL of diethylene glycol were added to the above mixture to obtain a deep blue solution. The vial was next placed on a preheated hot plate (300 °C) with vigorous stirring. After turning into green color, the mixture of $NiO_x$ and $MoO_x$ was then cooled by water, centrifuged, washed three times with water and acetone, and dried at 60 °C overnight. To obtain NiMo nanoparticles, the obtained precursors were reduced at 500 °C for 60 min with a temperature ramping of 10 °C/min under a gas flow of 10 sccm $H_2$/90 sccm Ar. After cooling to room temperature, the nanoparticles were passivated in air for several minutes before fully withdrawing the quartz boat from the furnace.

For modification with different amines, 10 mg of NiMo nanoparticles was dispersed in 5 mL of isopropanol by ultrasonication, followed by adding 100 μL (for liquids or 100 mg for solids) of amines. The mixture was stirred overnight, washed several times with ethanol to remove extra amines, and then dried in vacuum at 50 °C. A blank NiMo sample without adding any amines was also prepared in isopropanol as a control. Liquids of ethylamine (EA), EDA, dodecylamine (DDA), and hexanediamine (HDA) as well as a solid of 1,12-dodecanediamine (DDDA) were used in this work.

**2.2. Characterization.** The morphology of the NiMo nanoparticles was examined on a Hitachi-7700 transmission electron microscopy (TEM) instrument with an accelerating voltage of 120 kV. High-resolution TEM (HRTEM) images and selected area electron diffraction (SAED) patterns were obtained on an FEI Tecnai G2 S-TWIN microscope with an accelerating voltage of 200 kV. Powder X-ray diffraction (XRD) patterns were obtained using a Rigaku powder X-ray diffractometer with Cu Kα irradiation. Fourier transform infrared (FTIR) analyses were carried out using a Thermo Scientific Nicolet 6700 FTIR spectroscopy instrument. X-ray photoelectron spectra (XPS) were obtained using a Thermo Electron model K-Alpha spectrometer with Al Kα as the excitation source.

**2.3. Electrochemical Measurements.** To prepare the catalyst ink, 5 mg of electrocatalysts was dispersed in a mixture solution of 768 μL of deionized water, 200 μL of ethanol, and 32 μL of Nafion solution (5 wt %) by ultrasonication. Later, 5 μL of the as-prepared ink was dropped on a glass carbon (GC) electrode and dried naturally, with a loading density of 0.35 mg $cm^{-2}$. All electrochemical measurements were tested in 1 M KOH solution using a CHI 660D electrochemical workstation. A three-electrode system was set up to test the electrochemical properties of the NiMo-based electrocatalysts. GC electrode-supported catalysts, an Ag/AgCl (3 M KCl) electrode, and a graphite plate functioned as the working electrode, reference electrode, and counter electrode, respectively, in this system. To learn the activity of different catalysts, linear sweeping voltammetry analysis was carried out at a scan rate of 5 mV/s. The electrochemical impedance spectra (EIS) were obtained under a bias potential of 100 mV within the frequency range of 100 kHz to 0.1 Hz. With respect to reversible hydrogen electrode (RHE), the potential scale was corrected by the Nernst equation, where $E_{\text{versus RHE}} = E_{\text{versus Ag/AgCl}} + 0.0592 \times \text{pH} + 0.197$ V. All measurements were iR-corrected unless otherwise noted. The generated amount of hydrogen was evaluated under a fixed current density of 50 mA $cm^{-2}$, using gas chromatography (Techcomp GC 7900) with a thermal conductivity detector, and the faradaic efficiency was calculated from the measured amount of hydrogen and the theoretical value of hydrogen.

## 3. RESULTS AND DISCUSSION

Crystalline NiMo alloy nanoparticles were prepared via a previously reported method. Primary amines of EA and DDA as well as diamines of EDA, HDA, and DDDA were chosen to decorate the surface of the NiMo catalysts, as demonstrated in Figure 1a. The modified catalysts are denoted as "NiMo-x",

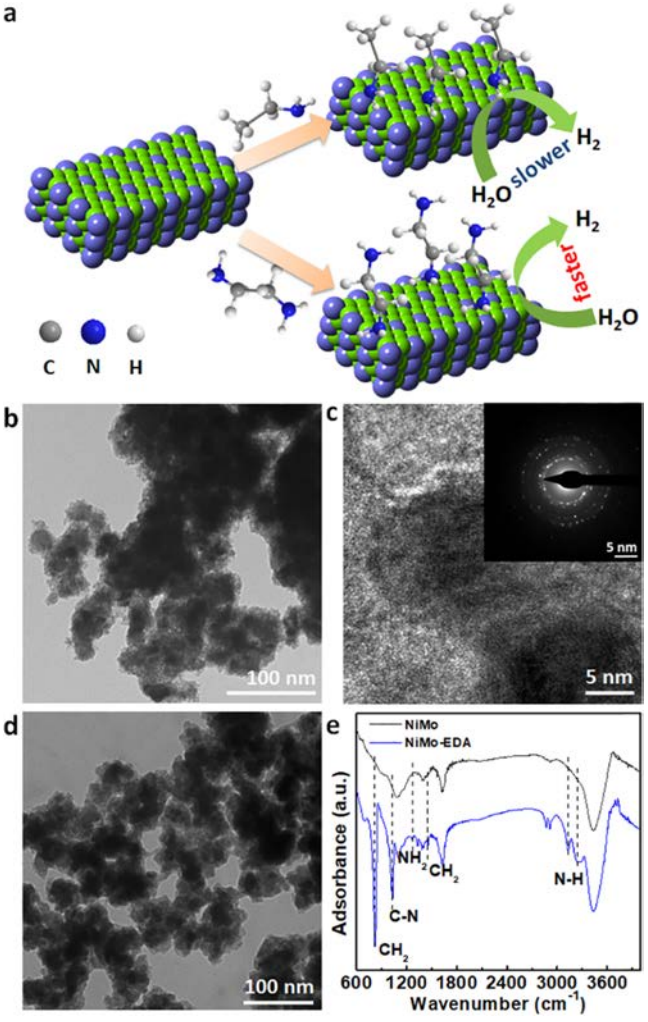


**Figure 1.** (a) Surface modification scheme of NiMo nanoparticles with various amines. (b) TEM image and (c) HRTEM image and SAED pattern of NiMo nanoparticles. (d) TEM image of NiMo-EDA nanoparticles. (e) FTIR spectra of NiMo and NiMo-EDA nanoparticles.

where x represents the names of amines. Typical TEM image in Figure 1b exhibited the aggregated nanoparticles of NiMo, whereas the HRTEM image and the SAED pattern in Figure 1c demonstrated the crystalline nature of the alloy. The XRD spectrum was also consistent with the above result (Figure S1), indexing to the $Ni_4Mo$ phase structure (JCPDS #65-5480).[30] To clarify the changes induced by the amine modification, characterizations on NiMo-EDA as a typical example were measured. After decorating with EDA, the particle-like morphology was well-preserved (Figure 1c). The XRD pattern


DOI: 10.1021/acsami.7b16125
ACS Appl. Mater. Interfaces 2018, 10, 1728−1733

(Figure S1), HRTEM image, and SAED pattern (Figure S2) of the NiMo nanoparticles present a crystal structure similar to that of the modified $Ni_4Mo$ alloy, suggesting that their structure and phase remain unaltered throughout the surface modification process.

The FTIR spectra of NiMo nanoparticles and NiMo-EDA were also collected to further illustrate the existence of the surface-adsorbed amine species (Figure 1d). The broad peak at 3437 $cm^{-1}$ is ascribed to the O−H stretching because of the absorbed water for both NiMo and NiMo-EDA.[32] Several new peaks were observed for NiMo-EDA as compared with that for NiMo. The peaks located at 817 and 1448 $cm^{-1}$ corresponded to the $CH_2$ rocking vibration, deformation in EDA, and stretching vibration of C−N bonds, whereas other peaks at 1264, 3132, and 3238 $cm^{-1}$ are attributed to the wag progression of $NH_2$, N−H symmetric stretching, and overtone of N−H deformation, correspondingly.[32−34] Thus, all results confirm the preserved morphology and crystallinity of the NiMo catalysts as well as the successful surface modification of EDA molecules.

The catalytic HER activities of the NiMo and amine-modified NiMo catalysts were then measured in 1.0 M KOH solution. The GC electrode as the support shows negligible HER activities in alkaline solutions (Figure 2a). For the primary amine-decorated NiMo catalysts, the polarization curves (with iR corrections) showed an apparent deterioration of activity for NiMo-EA and NiMo-DDA as compared with that of the pure NiMo nanoparticles. To reach the current density of 10 mA $cm^{-2}$, the NiMo nanoparticles required an overpotential of 340 mV, whereas those for NiMo-EA and NiMo-DDA were 414 and 469 mV, respectively, indicating that decorating with primary amines (EA and DDA) on the NiMo surface would have the HER catalytic activity decreased. In contrast, the NiMo-EDA electrocatalysts demonstrated a remarkable catalytic HER performance with a much smaller overpotential of 72 mV to reach 10 mA $cm^{-2}$, which was 268 mV lower than that of the unmodified NiMo catalysts. Further electrochemical analyses in Figure 2b−d illustrate the differences in the HER kinetics of NiMo with various surface decorations. As shown in Figure 2b, the derived Tafel slope of NiMo-EDA was 89 mV/dec, which was much lower than those of NiMo (135 mV/dec), NiMo-EA (143 mV/dec), and NiMo-DDA (155 mV/dec). To assess the actual difference of the active catalytic sites of NiMo modified with various amines, the double-layer capacitance ($C_{dl}$), proportional to the electrochemically active surface area (ECSA), was calculated. From cyclic voltammetry (CV) curves (Figure S3a−d) and their dependence plots (Figure 2c), both NiMo-EA (0.32 mF $cm^{-2}$) and NiMo-DDA (0.27 mF $cm^{-2}$) showed smaller $C_{dl}$ values as compared with that of NiMo (0.37 mF $cm^{-2}$). On the other hand, the $C_{dl}$ value of NiMo-EDA (16.3 mF $cm^{-2}$) was far larger than those of others, exhibiting decreased amounts of active sites by decorating EA and DDA but an increased quantity of sites by EDA modification. The EIS in Figure 2d clearly indicate the changes in the charge-transfer resistances ($R_{ct}$), where both NiMo-EA and NiMo-DDA yield larger $R_{ct}$, whereas NiMo-EDA displays a much smaller $R_{ct}$ as compared with that of NiMo. Therefore, all of these findings designate the adverse effect of modifying primary amines on NiMo surfaces by hindering their catalytic activity with slower kinetics and worse charge transfer but the apparent enhancement by decorating EDA to prominently facilitate the HER process.

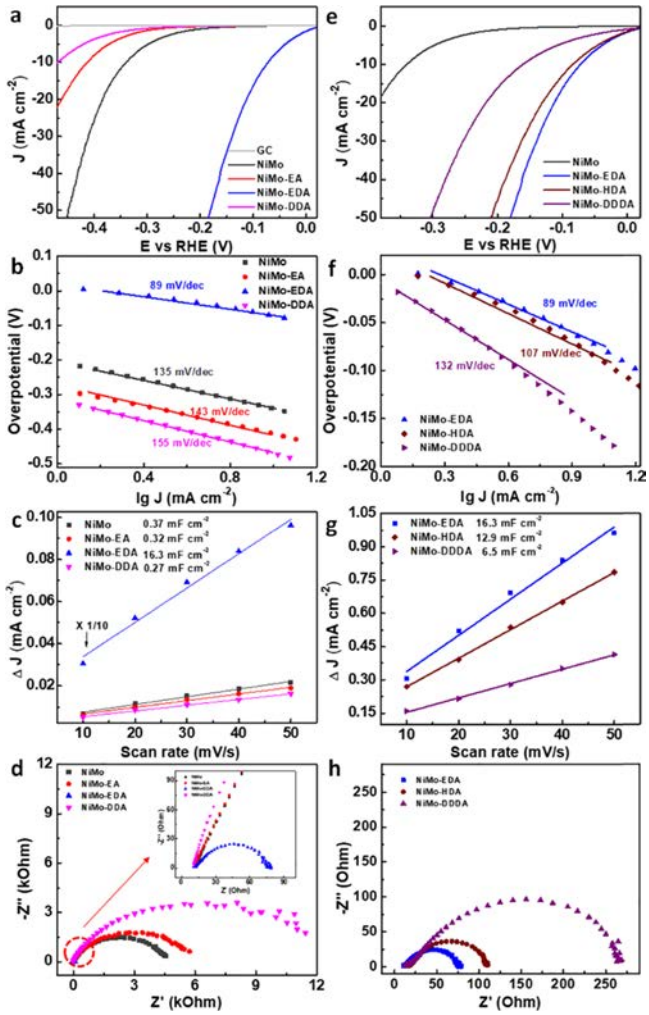


**Figure 2.** Electrochemical activity of the NiMo and amine-modified NiMo catalysts in 1.0 M KOH. (a,e) Catalytic activity for HER (with iR corrections). (b,f) Tafel slopes derived from (a,e). (c,g) $C_{dl}$ obtained from CV curves. (d,h) Nyquist plots.

As demonstrated with the substantial catalytic HER improvement on the NiMo catalysts by EDA surface modification, various diamines with different aliphatic amine chains, such as EDA, HDA, and DDDA, were then selected to further understand their insights on the activity enhancement. Polarization curves (with iR corrections) reveal that all diamine-modified NiMo catalysts show the improved HER activity as compared with that of the NiMo nanoparticles (Figure 2e). The overpotentials to drive the current density of 10 mA $cm^{-2}$ were 72, 85, and 161 mV for NiMo-EDA, NiMo-HDA, and NiMo-DDDA, respectively. The derived Tafel slopes (Figure 2f) of NiMo-HDA and NiMo-DDDA were 107 and 132 mV/dec, respectively, which are much larger than that of NiMo-EDA (89 mV/dec). Moreover, NiMo-EDA also had a much larger exchange current density of 1.888 mA $cm^{-2}$ as compared with those of NiMo (0.044 mA $cm^{-2}$), NiMo-HDA (1.629 mA $cm^{-2}$), and NiMo-DDDA (0.933 mA $cm^{-2}$). Differences in the overpotentials, Tafel slopes, and exchange current densities (Table S1) indicate the benefits and variation of the diamine-modified NiMo accompanied with the decreasing molecular chain length. Similarly, the values of $C_{dl}$ in Figure 2g calculated from the CV curves (Figure S3d−f) also exhibit a similar trend that NiMo-EDA (16.3 mF $cm^{-2}$) has the


DOI: 10.1021/acsami.7b16125
ACS Appl. Mater. Interfaces 2018, 10, 1728−1733

largest capacitance, followed by NiMo-HDA (12.9 mF $cm^{-2}$) and NiMo-DDDA (6.5 mF $cm^{-2}$). In addition, the charge-transfer resistances for the diamine-modified NiMo are smaller than those of the unmodified NiMo. Among them, NiMo-EDA has the smallest resistance (Figure 2h). Consequently, all of the diamine decoration can strengthen the catalytic HER activity of NiMo catalysts and their enhancement contributions would decrease gradually along with the chain length.

It is also important to investigate the catalytic stability for practical utilizations. The unmodified NiMo nanoparticles showed a stable current density of ~10.8 mA $cm^{-2}$ without significant fluctuations for 100 h under an overpotential of 350 mV (Figure 3). For the NiMo-EDA catalysts, a drop in the

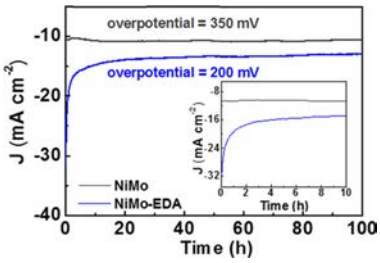


**Figure 3.** Catalytic stability of NiMo and NiMo-EDA in 1.0 M KOH. All measurements were performed without iR corrections.

catalytic current density under the overpotential of 200 mV was first observed within the initial several hours and then tended to be stable at ~13.5 mA $cm^{-2}$. The subsequent testing period of over 95 h witnessed their excellent stability under the overpotential of 200 mV, which is much larger than that of the NiMo catalysts at an even larger overpotential of 350 mV. Besides, the NiMo-EDA catalysts also displayed a good stability at a much higher current density of ~70 mA $cm^{-2}$ for 100 h under an overpotential of 300 mV (Figure S4). Additionally, the NiMo-EDA sample showed a faradaic efficiency of >99% during the HER process (Figure S5).

To shed light on the changes in the catalytic activity of NiMo-EDA during the stability test, FTIR and XPS were employed to examine their surface chemistry and oxidation states at various HER time intervals (5, 10, 30, and 60 min). FTIR spectra results in Figure 4a reveal the suppression in the characteristic peaks of EDA with increasing HER time, suggesting the gradual detachment of the physically adsorbed and loosely bonded EDA molecules from the NiMo surface. This is consistent with the decreased catalytic HER activity at the initial stage, as shown in Figure 3. After a duration of 10 h, because the peaks of EDA for NiMo-EDA were too weak to confirm the existence of EDA on the NiMo surface by FTIR (Figure S6), the surface chemical states of NiMo and NiMo-EDA before and after the 10 h tests were examined by XPS. The as-synthesized NiMo-EDA catalysts show a downshift of ~0.4 eV in the binding energies of both Ni 2p and Mo 3d as compared with those of NiMo (Figure 4b,c), suggesting the modulated oxidation states of NiMo by amine modifications. After 10 h of HER, there is not any evident change in the spent NiMo-EDA catalysts, which still give a peak downshift of ~0.4 eV as compared with that of the unmodified NiMo catalysts. This confirms the existence of EDA on the NiMo surface after a long-term catalytic reaction. Also, no apparent signal of nitrogen was observed for the unmodified NiMo, but the clear peak of N 1s for the used NiMo-EDA catalysts after the 10

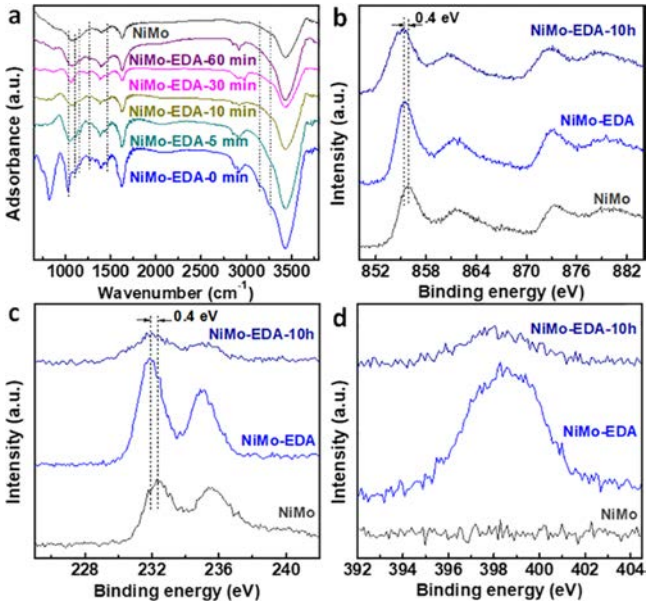


**Figure 4.** (a) FTIR spectra of NiMo-EDA at various HER time intervals for stability tests. XPS spectra of (b) Ni 2p, (c) Mo 3d, and (d) N 1s.

h test illustrated the residual strongly bonded EDA molecules on the NiMo surface (Figure 4d). Therefore, the stable current density in the case of NiMo-EDA after several hours of testing can be ascribed to the tightly chemical-bonded EDA on the NiMo surfaces.

Regarding the combination form between amines and NiMo catalysts, it could be attributed to the interaction between the N atom of the amino group of various amines and the metal surface. Specifically, the N atom in the amino group has one lone pair of electrons, whereas the metal atoms of both Ni and Mo have unoccupied d-orbitals; therefore, when they meet together, the donation of the lone pair of electrons from N to d-orbitals of metals would lead to the formation of coordination bonds between N and metals, which is well-consistent with the classic Lewis acid−base concept. In contrast, because both C and H atoms do not have lone pair of electrons, their interactions with metals would be very weak and unstable. Moreover, according to the previous study,[34,35] the N atom of the amine group has been confirmed to be directly coordinated to the metal surface without protonated amino groups. Similarly, the direct bonding of N atom in amines with metals in other compounds is also reported.[19,32] Also, after the formation of monolayers of amines on the metal surface through chemical bonding, the multiple layers of amines should also be adsorbed physically. These physically adsorbed layers of amines can be desorbed by washing or during the catalytic process, which is consistent with the gradually decreased catalytic activity (Figure 3), which can be further confirmed by FTIR spectra (Figure 4a). In any case, the first layer or monolayer of amines on the metal surface is anticipated to be stable during washing and catalytic reactions, where this stability is well-observed during the catalytic performance evaluation of the modified NiMo catalysts (Figure 3) and XPS measurement of the catalysts operated for 10 h (Figure 4b−d).

Many works have illustrated the catalytic enhancement by removing the surface-adsorbed organic ligands to avoid the site blockage and to promote the accessibility of the catalyst surface.[17,19] Cossairt et al. reported that DDA on the surface of


DOI: 10.1021/acsami.7b16125
ACS Appl. Mater. Interfaces 2018, 10, 1728−1733

$WSe_2$ would block the surface catalytic centers, reducing the HER activity and kinetics, but the removal of DDA could recover its catalytic activity.[19] Being consistent with the previous findings, our results clearly demonstrate that decorating primary amines on NiMo, regardless of their chain length, results in the suppression of the HER catalytic activity because of the blockage of active surface sites, which can be justified by asmaller ECSA and slower kinetics of HER with larger Tafel slopes and higher charge-transfer resistances. Because of the relatively large Tafel slopes for all amine-modified NiMo catalysts, the HER pathway would undergo the Volmer–Heyrovsky process in alkaline solutions.[3,36] Furthermore, because alkyl groups (e.g., $C_2H_5-$ and $C_{12}H_{25}-$ in this work) are hydrophobic to inhibit water adsorption[37] and the steric hindrance of long alkyl chains also prevent the access of water molecules,[23] the Volmer reaction (electroreduction of water molecules with hydrogen adsorption, $M + H_2O + e^- \rightarrow MH_{ads} + OH^-$) and Heyrovsky reaction (electrochemical hydrogen desorption, $MH_{ads} + H_2O + e^- \rightarrow M + H_2 + OH^-$) for the primary amine-decorated NiMo would be sluggish, leading to a decreased catalytic performance.

On the contrary, the positive effects of diamines have been examined to facilitate the HER process with lower overpotentials, smaller Tafel slopes, larger ECSA, and more efficient charge transfers (Figure 2e–h). For the NiMo-EDA electrocatalysts, the amino groups bounded to the NiMo surface would donate electrons to NiMo, leading to an electron-rich surface to accelerate the HER process. As given in Figure 4b,c, both Ni and Mo of NiMo-EDA show the downshift of ~0.4 eV in the binding energy as compared with those of NiMo, suggesting the electron-rich state of the NiMo surface by accepting electrons from amino groups in EDA. The catalytic activities are also closely dependent on the interface properties (e.g., wettability) between the electrolyte and the electrode for specific electrocatalysts.[17,19] As a consequence, the free amino group in EDA for the EDA-modified NiMo can further help the adsorption of water molecules and their transportation to the NiMo surface.[38,39] Therefore, using diamines to decorate the NiMo surface can enhance their HER catalytic performance remarkably because of the modified surfaces with an electron-rich state, better conductivity, and easier access of water. Interestingly, for both primary amine- and diamine-modified NiMo, the longer aliphatic chains of amines, the poorer HER activity of the modified NiMo is observed, which may be related to the steric hindrance effect of the aliphatic chains.[20,36] In any case, as analyzed above, the diamine-modified NiMo electrocatalysts still perform much better than the unmodified NiMo nanoparticles.

## 4. CONCLUSIONS

In summary, a novel and facile approach to modulate and engineer the interface properties of the NiMo electrocatalysts by decorating diamines was proposed and successfully demonstrated. The influence of the amino groups and their chain length on the catalytic properties for HER in alkaline media was investigated. Primary amine-modified catalysts exhibited a weaker activity with slower kinetics, whereas diamine-decorated ones displayed significantly improved activity and kinetics because of the benefits of electron-rich surface and small resistance. With the longer molecular length, both primary amines and diamines display a similar trend with declining electrochemical activities, but catalytic performances of the diamine-modified NiMo catalysts are still better than those of the unmodified ones. This method may provide a valuable strategy to engineer the electrolyte–electrode interface with surface modification of electrocatalysts with the aim to enhance their catalytic performance.

## ■ ASSOCIATED CONTENT

### Supporting Information

The Supporting Information is available free of charge on the ACS Publications website at DOI: 10.1021/acsami.7b16125.

Detailed information including XRD patterns; TEM image, HRTEM image, and SAED pattern; CV curves; stability test; faradaic efficiency; and FTIR spectra of NiMo, NiMo-EA, and NiMo-EDA (PDF)

## ■ AUTHOR INFORMATION


### Corresponding Authors

*E-mail: johnnyho@cityu.edu.hk (J.C.H.).
*E-mail: yyma@mail.xjtu.edu.cn (Y.M.).
*E-mail: yongquan@mail.xjtu.edu.cn (Y.Q.).

### ORCID

Johnny C. Ho: 0000-0003-3000-8794
Yongquan Qu: 0000-0002-6202-1929


### Notes

The authors declare no competing financial interest.

## ■ ACKNOWLEDGMENTS

Authors acknowledge the financial support from the National 1000-Plan program, the National Natural Science Foundation of China (grant nos. 21401148 and 51672229), the Science Technology and Innovation Committee of Shenzhen Municipality (grant no. JCYJ20160229165240684), and the Environment and Conservation Fund of Hong Kong SAR, China (ECF 2016-85). Y.Q. is also supported by the Cyrus Tang Foundation through Tang Scholar Program.

## ■ REFERENCES


(1) Seh, Z. W.; Kibsgaard, J.; Dickens, C. F.; Chorkendorff, I.; Nørskov, J. K.; Jaramillo, T. F. Combining theory and experiment in electrocatalysis: Insights into materials design. *Science* **2017**, *355*, No. eaad4998.

(2) Chu, S.; Cui, Y.; Liu, N. The path towards sustainable energy. *Nat. Mater.* **2017**, *16*, 16–22.

(3) Wang, J.; Xu, F.; Jin, H.; Chen, Y.; Wang, Y. Non-noble metal-based carbon composites in hydrogen evolution reaction: fundamentals to applications. *Adv. Mater.* **2017**, *29*, 1605838.

(4) Shi, Y.; Zhang, B. Recent advances in transition metal phosphide nanomaterials: synthesis and applications in hydrogen evolution reaction. *Chem. Soc. Rev.* **2016**, *45*, 1529–1541.

(5) Roger, I.; Shipman, M. A.; Symes, M. D. Earth-abundant catalysts for electrochemical and photoelectrochemical water splitting. *Nat. Rev. Chem.* **2017**, *1*, 0003.

(6) Anantharaj, S.; Ede, S. R.; Sakthikumar, K.; Karthick, K.; Mishra, S.; Kundu, S. Recent Trends and Perspectives in Electrochemical Water Splitting with an Emphasis on Sulfide, Selenide, and Phosphide Catalysts of Fe, Co, and Ni: A Review. *ACS Catal.* **2016**, *6*, 8069–8097.

(7) Xiao, P.; Chen, W.; Wang, X. A review of phosphide-based materials for electrocatalytic hydrogen evolution. *Adv. Energy Mater.* **2015**, *5*, 1500985.

(8) Safizadeh, F.; Ghali, E.; Houlachi, G. Electrocatalysis developments for hydrogen evolution reaction in alkaline solutions—a review. *Int. J. Hydrogen Energy* **2015**, *40*, 256–274.

(9) Meng, Y.; Song, W.; Huang, H.; Ren, Z.; Chen, S.-Y.; Suib, S. L. Structure–property relationship of bifunctional $MnO_2$ nanostructures:




DOI: 10.1021/acsami.7b16125
*ACS Appl. Mater. Interfaces* 2018, 10, 1728–1733

highly efficient, ultra-stable electrochemical water oxidation and oxygen reduction reaction catalysts identified in alkaline media. *J. Am. Chem. Soc.* **2014**, *136*, 11452−11464.
(10) Yang, J.; Zhang, F.; Wang, X.; He, D.; Wu, G.; Yang, Q.; Hong, X.; Wu, Y.; Li, Y. Porous molybdenum phosphide nano-octahedrons derived from confined phosphorization in UIO-66 for efficient hydrogen evolution. *Angew. Chem., Int. Ed.* **2016**, *55*, 12854−12858.
(11) Zhang, X.; Liu, S.; Zang, Y.; Liu, R.; Liu, G.; Wang, G.; Zhang, Y.; Zhang, H.; Zhao, H. $Co/Co_9S_8$@S, N-doped porous graphene sheets derived from S, N dual organic ligands assembled Co-MOFs as superior electrocatalysts for full water splitting in alkaline media. *Nano Energy* **2016**, *30*, 93−102.
(12) Tang, C.; Wang, W.; Sun, A.; Qi, C.; Zhang, D.; Wu, Z.; Wang, D. Sulfur-decorated molybdenum carbide catalysts for enhanced hydrogen evolution. *ACS Catal.* **2015**, *5*, 6956−6963.
(13) Jia, X.; Zhao, Y.; Chen, G.; Shang, L.; Shi, R.; Kang, X.; Waterhouse, G. I. N.; Wu, L.-Z.; Tung, C.-H.; Zhang, T. $Ni_3FeN$ nanoparticles derived from ultrathin NiFe-layered double hydroxide nanosheets: an efficient overall water splitting electrocatalyst. *Adv. Energy Mater.* **2016**, *6*, 1502585.
(14) Li, J.; Yan, M.; Zhou, X.; Huang, Z.-Q.; Xia, Z.; Chang, C.-R.; Ma, Y.; Qu, Y. Mechanistic insights on ternary $Ni_{2-x}Co_xP$ for hydrogen evolution and their hybrids with graphene as highly efficient and robust catalysts for overall water splitting. *Adv. Funct. Mater.* **2016**, *26*, 6785−6796.
(15) Gao, W.; Yan, M.; Cheung, H.-Y.; Xia, Z.; Zhou, X.; Qin, Y.; Wong, C.-Y.; Ho, J. C.; Chang, C.-R.; Qu, Y. Modulating electronic structure of CoP electrocatalysts towards enhanced hydrogen evolution by Ce chemical doping in both acidic and basic media. *Nano Energy* **2017**, *38*, 290−296.
(16) Cheung, H.-Y.; Yip, S.; Han, N.; Dong, G.; Fang, M.; Yang, Z.-x.; Wang, F.; Lin, H.; Wong, C.-Y.; Ho, J. C. Modulating electrical properties of InAs nanowires via molecular monolayers. *ACS Nano* **2015**, *9*, 7545−7552.
(17) Li, D.; Wang, C.; Tripkovic, D.; Sun, S.; Markovic, N. M.; Stamenkovic, V. R. Surfactant removal for colloidal nanoparticles from solution synthesis: the effect on catalytic performance. *ACS Catal.* **2012**, *2*, 1358−1362.
(18) Lu, S.; Zhuang, Z. Investigating the influences of the adsorbed species on catalytic activity for hydrogen oxidation reaction in alkaline electrolyte. *J. Am. Chem. Soc.* **2017**, *139*, 5156−5163.
(19) Henckel, D. A.; Lenz, O.; Cossairt, B. M. Effect of ligand coverage on hydrogen evolution catalyzed by colloidal $WSe_2$. *ACS Catal.* **2017**, *7*, 2815−2820.
(20) Kan, K.; Xia, T.; Li, L.; Bi, H.; Fu, H.; Shi, K. Amidation of single-walled carbon nanotubes by a hydrothermal process for the electrooxidation of nitric oxide. *Nanotechnology* **2009**, *20*, 185502.
(21) Murugesan, S.; Myers, K.; Subramanian, V. Amino-functionalized and acid treated multi-walled carbon nanotubes as supports for electrochemical oxidation of formic acid. *Appl. Catal., B* **2011**, *103*, 266−274.
(22) Cao, H.; Wu, X.; Yin, G.; Warner, J. H. Synthesis of adenine-modified reduced graphene oxide nanosheets. *Inorg. Chem.* **2012**, *51*, 2954−2960.
(23) Xu, J.; Jia, G.; Mai, W.; Fan, H. J. Energy storage performance enhancement by surface engineering of electrode materials. *Adv. Mater. Interfaces* **2016**, *3*, 1600430.
(24) Xu, G.-R.; Bai, J.; Yao, L.; Xue, Q.; Jiang, J.-X.; Zeng, J.-H.; Chen, Y.; Lee, J.-M. Polyallylamine-functionalized platinum tripods: enhancement of hydrogen evolution reaction by proton carriers. *ACS Catal.* **2017**, *7*, 452−458.
(25) Lu, Z.; Xu, W.; Ma, J.; Li, Y.; Sun, X.; Jiang, L. Superaerophilic carbon-nanotube-array electrode for high-performance oxygen reduction reaction. *Adv. Mater.* **2016**, *28*, 7155−7161.
(26) Li, Y.; Zhao, C. Enhancing water oxidation catalysis on a synergistic phosphorylated NiFe hydroxide by adjusting catalyst wettability. *ACS Catal.* **2017**, *7*, 2535−2541.
(27) Li, S.; Yu, C.; Yang, J.; Zhao, C.; Zhang, M.; Huang, H.; Liu, Z.; Guo, W.; Qiu, J. A Superhydrophilic "nanoglue" for stabilizing metal hydroxides onto carbon materials for high-energy and ultralong-life asymmetric supercapacitors. *Energy Environ. Sci.* **2017**, *10*, 1958−1965.
(28) Liu, L.; Zha, D.-W.; Wang, Y.; He, J.-B. A nitrogen- and sulfur-rich conductive polymer for electrocatalytic evolution of hydrogen in acidic electrolytes. *Int. J. Hydrogen Energ* **2014**, *39*, 14712−14719.
(29) McKone, J. R.; Sadtler, B. F.; Werlang, C. A.; Lewis, N. S.; Gray, H. B. Ni−Mo nanopowders for efficient electrochemical hydrogen evolution. *ACS Catal.* **2013**, *3*, 166−169.
(30) Wang, Y.; Zhang, G.; Xu, W.; Wan, P.; Lu, Z.; Li, Y.; Sun, X. A 3D nanoporous Ni-Mo electrocatalyst with negligible overpotential for alkaline hydrogen evolution. *ChemElectroChem* **2014**, *1*, 1138−1144.
(31) Fang, M.; Gao, W.; Dong, G.; Xia, Z.; Yip, S.; Qin, Y.; Qu, Y.; Ho, J. C. Hierarchical NiMo-based 3D electrocatalysts for highly-efficient hydrogen evolution in alkaline conditions. *Nano Energy* **2016**, *27*, 247−254.
(32) Xu, D.; Liu, Z.; Liang, J.; Qian, Y. Solvothermal synthesis of CdS nanowires in a mixed solvent of ethylenediamine and dodecanethiol. *J. Phys. Chem. B* **2005**, *109*, 14344−14349.
(33) Deng, Z.-X.; Li, L.; Li, Y. Novel inorganic−organic-layered structures: crystallographic understanding of both phase and morphology formations of one-dimensional CdE (E=S, Se, Te) nanorods in ethylenediamine. *Inorg. Chem.* **2003**, *42*, 2331−2341.
(34) Kim, J.; Jung, D.; Park, Y.; Kim, Y.; Moon, D. W.; Lee, T. G. Quantitative analysis of surface amine groups on plasma-polymerized ethylenediamine films using UV−visible spectroscopy compared to chemical derivation with FT-IR spectroscopy, XPS and TOF-SIMS. *Appl. Surf. Sci.* **2007**, *253*, 4112−4118.
(35) Incorvio, M. J.; Contarini, S. X-ray photoelectron spectroscopic studies of metal/inhibitor systems: structure and bonding at the iron/amine interface. *J. Electrochem. Soc.* **1989**, *136*, 2493−2498.
(36) Zheng, Y.; Jiao, Y.; Jaroniec, M.; Qiao, S. Z. Advancing the electrochemistry of the hydrogen-evolution reaction through combining experiment and theory. *Angew. Chem., Int. Ed.* **2015**, *54*, 52−65.
(37) Honda, M.; Oaki, Y.; Imai, H. Hydrophobic inorganic−organic composite nanosheets based on monolayers of transition metal oxides. *Chem. Mater.* **2014**, *26*, 3579−3585.
(38) Wang, S.; Wang, J.; Zhang, W.; Ji, J.; Li, Y.; Zhang, G.; Zhang, F.; Fan, X. Ethylenediamine modified graphene and its chemically responsive supramolecular hydrogels. *Ind. Eng. Chem. Res.* **2014**, *53*, 13205−13209.
(39) Li, Z.; Zabihi, O.; Wang, J.; Li, Q.; Wang, J.; Lei, W.; Naebe, M. Hydrophilic PAN based carbon nanofibres with improved graphitic structure and enhanced mechanical performance using ethylenediamine functionalized graphene. *RSC Adv.* **2017**, *7*, 2621−2628.


DOI: 10.1021/acsami.7b16125
*ACS Appl. Mater. Interfaces* 2018, 10, 1728−1733